NASA TECHNICAL MEMORANDUM

NASA TM X-71971

COPY NO.

NASA TM X-71971

(NASA-TM-X-71971) A FOREBODY DESIGN TECHNIQUE FOR HIGHLY INTEGRATED BOTTOM-MOUNTED SCRAMJETS WITH APPLICATION TO A HYPERSONIC RESEARCH AIRPLANE (NASA) 40 p HC $3.75 CSCL 21A

N75-11973

Unclas

G3/07 03626

A FOREBODY DESIGN TECHNIQUE FOR HIGHLY INTEGRATED BOTTOM-MOUNTED SCRAMJETS WITH APPLICATION TO A HYPERSONIC RESEARCH AIRPLANE

C.L.W.EDWARDS

LANGLEY RESEARCH CENTER

NOV. 1974

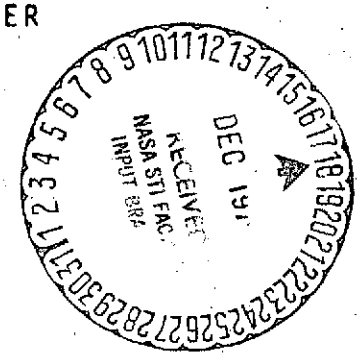

NATIONAL AERONAUTICS AND SPACE ADMINISTRATION

LANGLEY RESEARCH CENTER, HAMPTON, VIRGINIA 23665

1. Report No.	2. Government Accession No.	3. Recipient's Catalog No.
TM X-71971		

4. Title and Subtitle	5. Report Date
A FOREBODY DESIGN TECHNIQUE FOR HIGHLY INTEGRATED BOTTOM-MOUNTED SCRAMJETS WITH APPLICATION TO A HYPERSONIC RESEARCH AIRPLANE	Nov. 1974
	6. Performing Organization Code
7. Author(s)	8. Performing Organization Report No.
C. L. W. Edwards	
9. Performing Organization Name and Address	10. Work Unit No.
Langley Research Center Hampton, Virginia 23665	11. Contract or Grant No.
	13. Type of Report and Period Covered
12. Sponsoring Agency Name and Address	Technical Memorandum
National Aeronautics & Space Administration Washington, D. C. 20546	14. Sponsoring Agency Code

15. Supplementary Notes

Interim technical information release, subject to possible revision and/or later formal publication.

16. Abstract

A rapid and simple inviscid technique for designing forebodies which produce uniformly precompressed flows at the inlet entrance for bottom-mounted scramjets has been developed so that geometric constraints resulting from design trade-offs can be effectively evaluated. The flow fields resulting from several forebody designs generated in support of a hypersonic research airplane conceptual design study have been analyzed in detail with three-dimensional characteristics calculations to verify the uniform flow conditions. For the designs analyzed, uniform flow is maintained over a wide range of flight conditions (M=4 to 10; α=6° to 10°) corresponding to scramjet operation flight envelope of the research airplane.

17. Key Words (Suggested by Author(s)) (STAR category underlined)	18. Distribution Statement
°Forebody Design °Scramjets °Uniform Flow °Engine/Airframe Integration °Inlet Flows °Precompression	Unclassified - unlimited

19. Security Classif. (of this report)	20. Security Classif. (of this page)	21. No. of Pages	22. Price*
Unclassified	Unclassified	38	$3.75

*Available from { The National Technical Information Service, Springfield, Virginia 22151
STIF/NASA Scientific and Technical Information Facility, P.O. Box 33, College Park, MD 20740

A FOREBODY DESIGN TECHNIQUE FOR HIGHLY INTEGRATED BOTTOM-MOUNTED SCRAMJETS WITH APPLICATION TO A HYPERSONIC RESEARCH AIRPLANE

C.L.W.Edwards

Langley Research Center

SUMMARY

The efficiency of future hypersonic airbreathing aircraft will depend to a great extent on the maximum integration of the propulsion system with the vehicle airframe. A rapid and simple inviscid technique for designing forebodies which produce uniformly precompressed flows at the inlet entrance for bottom-mounted scramjets has been developed so that geometric constraints resulting from design trade-offs can be effectively evaluated. The flow fields resulting from several forebody designs generated in support of a hypersonic research airplane conceptual design study have been analyzed in detail with three-dimensional characteristics calculations to verify the uniform flow conditions. For the designs analyzed, uniform flow is maintained over a wide range of flight conditions corresponding to scramjet operation flight envelope of the research airplane.

INTRODUCTION

A large spectrum of promising future military and civil applications of hydrogen-fueled airbreathing aircraft for high supersonic and hypersonic flight has been well documented in the literature (refs. 1-5). A common feature of these aircraft is the necessity to carefully integrate the propulsion system with the vehicle airframe to obtain optimum overall performance. As shown

in figure 1, the size of the propulsion system relative to aircraft size increases rapidly with increasing flight Mach number and the forces, as discussed in reference 6, generated by the propulsion system become large compared to aerodynamic forces. The mutual interactions between these large forces can be advantageous when the propulsion system is properly integrated with the vehicle airframe. Thus, the engine/airframe integration process represents a major design opportunity to maximize the performance of hypersonic airbreathing vehicles.

The highly integrated aircraft concepts depicted in figure 1 are attractive because they provide maximum inlet capture area and nozzle expansion area while maintaining minimum cowl drag. However, to take full advantage of this arrangement, the vehicle propulsion system must be properly integrated early in the design process. Some interactive constraints which must be considered in the design of highly integrated hypersonic systems are shown in figure 2. The size and number of the engines must be sufficient to meet mission requirements. The scramjet inlet must be located within the forebody compression field to obtain maximum performance. An effective precompression tends to reduce the physical dimensions of the inlet, in which turn tends to reduce engine weight and cowl drag. If the precompressed flow at the inlet face can also be made uniform, then the increased complexity in inlet design required for efficient operation in widely varying flows can also be alleviated. However, the available shock layer capture area decreases with Mach number, so that it becomes necessary for the inlet to capture most of the flow between the body and the bow shock across the entire fuselage span. The

engine size and the flow field requirements are not the only considerations necessary for a good forebody design. Aerodynamic, structural and internal volume requirements must also be incorporated as early design constraints to achieve an optimum configuration.

The scramjet nozzle design is primarily governed by thrust and stability requirements. Thus, the location of the scramjet, orientation of the thrust vector, and the resulting trim penalties must be examined across the entire flight envelope (ref. 6). The strong interaction between the nozzle exhaust and the nonuniform flows surrounding the vehicle afterbody and external cowl must also be accounted for in evaluation of nozzle performance.

It is apparent, therefore, that one key to optimum vehicle performance is a systematic procedure for effectively assessing the interactive constraints early in the design if any realistic beneficial coupling between the engine and airframe is to be achieved. A significant research effort is being applied at Langley Research Center to examine, develop, and validate the technology necessary to perform such assessments during the design process on a routine basis. The engine-nozzle-vehicle interactions and design methodology are presented in reference 6. The primary objectives of this paper are to describe recent progress in forebody design methodology, present some results from a vehicle design study, and to indicate some areas of research which could enhance overall design capability.

SYMBOLS

A	forebody cross-sectional area
A_c	inlet capture area
D	axial design length of constant impact angle surface

H	inlet height
$\hat{i},\hat{j},\hat{k}$	unit vector components in x,y,z directions,respectively
M	Mach number
$\vec{n}$	outward unit normal surface vector
n_x,n_y,n_z	direction cosines of outward unit normal surface vector
P	static pressure
P,Q,R,S,T,SG	lofting curve coefficients for forebody geometry
r	radius of equivalent circular forebody cross-section
$\vec{S}$	surface tangent vector in Newtonian stream direction
S_{ref}	vehicle reference area
V	velocity
$\vec{V}$	velocity vector
$\frac{V_x}{\lvert V\rvert},\frac{V_y}{\lvert V\rvert},\frac{V_z}{\lvert V\rvert}$	direction cosines of velocity vector
$\vec{v}$	unit vector in velocity direction
x,y,z	forebody reference coordinates
α	angle-of-attack referenced to lower surface center-line of forebody at the inlet entrance
δ	Newtonian impact angle
θ_o	lower forebody center-line deflection angle
ρ	density
$\frac{\rho V}{\rho_\infty V_\infty}$	local to free-stream mass flow ratio
ϕ	forebody cross-section meridian angle
ψ	Mach angle, $\sin^{-1}\left(\frac{1}{M}\right)$

Subscripts

∞	free-stream conditions
2	local conditions
I	inlet
ℓ,m	indices for lofting line coefficients

Forebody Design Procedure

The forebody design goals are indicated in figure 3. The key flow parameters and the region at the inlet entrance requiring uniform precompression are also shown. The cross-sectional area (located at the inlet face) in which the flow is to be tightly constrained is bounded by the vehicle surface and two functions of engine geometry: (1) the position of the outboard engine module; and (2) the position of the cowl lip (or bow shock as the Mach number becomes large). This control area is represented by the cross-hatched region on figure 3. An ideal and probably unattainable design would render the oncoming precompressed flow parallel and uniform in the control area and remain invariant with changes in Mach number and angle of attack. The practical goals for this study were to develop a straightforward design procedure which can be used effectively to minimize gradients in key flow parameters in the region of the inlet entrance over the vehicle flight envelope.

The parameters which directly influence inlet and engine performance are the mass flow to be ingested, the static pressure, local Mach number and flow angularity. These parameters are sufficient to define the state of the flow and if they are uniform then it follows that the remaining flow variables will also be uniform. The most predominant of these parameters, which is a good approximate measure of forebody effectiveness, is the relative mass flow. A

reduction in mass flow would cause a corresponding reduction in thrust available from a fixed size engine and large gradients in mass flow would require complex fuel scheduling between engine modules to achieve maximum performance.

Computational techniques.- There are several numerical techniques which are capable of calculating supersonic inviscid flows over three-dimensional geometries (refs. 7-10). In principle, any of these techniques could be employed to derive a geometry which produces uniform flow at the inlet entrance. Either parametric studies of several geometries or an inverse approach using one of these techniques to directly solve for the appropriate geometric boundary could be employed. The parametric approach appears too restrictive and time consuming for the preliminary design process. The inverse technique can, in principle, be accomplished by specifying the inlet station flow conditions and performing an upwind numerical calculation (characteristics or finite difference) to solve for a geometry which maintains the specified flow. However, the resulting geometry could be very difficult to constrain so that required trade-offs could be performed on the basis of other multi-disciplinary functions of merit which must be considered to achieve a realistic optimum. The complexity required for this procedure does not seem warranted for the preliminary design task since one of the basic study goals was to develop a straightforward and rapid preliminary design tool. Therefore, the approach taken in this study is a very simplified analogy to the inverse technique where basic hypersonic flow relations are utilized in lieu of more exact numerical schemes to determine the appropriate forebody geometry.

Design Method.- At hypersonic speeds, Newtonian flow gives a good representation of the inviscid conditions on three-dimensional compression surfaces which do not produce strong cross flows or imbedded shocks. Since the shock layer is

thin, the surface conditions should also represent the conditions in the field if those surface conditions are everywhere uniform over the control area. In addition, the surface geodesics (defined in the classical sense as the shortest surface distance between two points) become streamlines when the surface pressure is constant. Therefore, the problem is one of creating a geometry from the Newtonian stream directions such that the Newtonian impact angle is a constant (figure 4).

The classic equation for the Newtonian impact angle (δ) in terms of the velocity vector

$$\vec{V} = V_x \hat{i} + V_y \hat{j} + V_z \hat{k} \tag{1}$$

and the outward normal to the surface

$$\vec{n} = n_x \hat{i} + n_y \hat{j} + n_z \hat{k} \tag{2}$$

is

$$\sin\delta = -\left(\frac{n_x V_x}{|V|} + \frac{n_y V_y}{|V|} + \frac{n_z V_z}{|V|}\right) \tag{3}$$

If the velocity vector is a function of angle of attack (α) only (no yaw), then a unit vector in the velocity direction can be defined by

$$\vec{v} = \cos\alpha \hat{j} + \sin\alpha \hat{k} \tag{4}$$

and the Newtonian impact angle becomes

$$\sin\delta = -(n_y \cos\alpha + n_z \sin\alpha) \tag{5}$$

Solving equation (5) for n_y and substituting into equation (2), the normal vector in terms of n_x and n_z becomes

$$\vec{n} = n_x \hat{i} - \left(\frac{n_z \sin\alpha + \sin\delta}{\cos\alpha}\right)\hat{j} + n_z \hat{k} \tag{6}$$

n_x can be determined from the local cross-section curve of the vehicle by relating its slope to the surface normal

$$n_x = -n_z \tan\phi \tag{7}$$

where

$$\tan\phi = \left(\frac{dz}{dx}\right) . \tag{8}$$

Substituting (7) into (6) we get

$$\vec{n} = -n_z \tan\phi \hat{i} - \left(\frac{n_z \sin\alpha + \sin\delta}{\cos\alpha}\right)\hat{j} + n_z \hat{k} \tag{9}$$

and since by definition

$$\vec{n} \cdot \vec{n} = n_x^2 + n_y^2 + n_z^2 = 1 \tag{10}$$

n_z can be determined in terms of the vehicle angle of attack, Newtonian impact angle, and cross-sectional geometry from equations (9) and (10).

$$n_z = \frac{-\sin\delta \sin\alpha - \cos\alpha\sqrt{\cos^2\delta + (\cos^2\alpha - \sin^2\delta)\tan^2\phi}}{1 + \cos^2\alpha \tan^2\phi} \tag{11}$$

The relations for n_x and n_y in terms of the same parameters become

$$n_x = \frac{[\sin\delta \sin\alpha + \cos\alpha\sqrt{\cos^2\delta + (\cos^2\alpha - \sin^2\delta)\tan^2\phi}]\tan\phi}{1 + \cos^2\alpha \tan^2\phi} \tag{12}$$

$$n_y = \frac{-\sin\delta\cos\alpha + \sin\alpha\sqrt{\cos^2\delta + (\cos^2\alpha - \sin^2\delta)\tan^2\phi}\ \cos^2\phi}{\cos^2\phi + \cos^2\alpha\sin^2\phi} \tag{13}$$

The geodesic directions are maintained coincident with the Newtonian stream direction ($\vec{S}$) which can be determined by taking successive vector products between the surface normal and the wind vector

$$\vec{S} = \vec{n} \times (\vec{n} \times \vec{v}) \tag{14}$$

as illustrated in the vector diagram of figure 4. Any number of geodesic directions can be determined along a given cross section and projected upstream some arbitrary distance, Δy. The locus of these projected geodesics can then be used to define a new upstream cross section and the process repeated until the desired surface is fully determined.

The preliminary design method illustrated here was developed for arbitrary forebody geometry; however, the numerical methods available to verify the flow fields are somewhat geometry restricted. Three-dimensional characteristic calculations using the computer program of reference 7 were used in this study to verify the design technique. This characteristics program is limited to smooth continuous geometries with bielliptic cross sections. However, general variation in the longitudinal direction is allowed, as illustrated in figure 5, by defining the projections of three lofting lines in the vehicle coordinate planes with a series of segments using the general conic

$$\begin{pmatrix} x \\ z \end{pmatrix}_{\ell,m} = P_{\ell,m}\, Y + Q_{\ell,m} + (SG)_{\ell,m}\sqrt{R_{\ell,m}\, Y^2 + S_{\ell,m}\, Y + T_{\ell,m}} \tag{15}$$

where $\ell = 1$, number of segments

and m=1, 6 corresponding to the six projections of the three lofting curves

on the coordinate planes.

Constant impact angle is not necessary over the entire undersurface of the forebody since influence at the inlet station from upstream geometry is not generally felt past a point where a Mach wave from the body intersects the cowl lip. This distance is illustrated in figure 5 and is the upstream boundary for which the forebody must be closely tailored. Since it is likely that the flow will not be entirely uniform between body and bow shock, the largest free stream Mach number in the vehicle flight envelope is used to specify the upstream boundary to ensure adequate design length, D, to develop uniform flow at the inlet face.

$$D = \frac{H}{\tan (\theta_o + \psi) - \tan \theta_o} \tag{16}$$

where θ_o is determined by the center-line slope

$$\theta_o = \tan^{-1}\left(\frac{dz}{dy}\right)_{C_L} \tag{17}$$

and ψ is the free-stream Mach angle

$$\psi = \sin^{-1}\left(\frac{1}{M_\infty}\right) \tag{18}$$

The lower center-line geodesic is kept straight over the design length but is allowed to curve upstream of this point to meet aerodynamic and volumetric constraints. However, care must be taken to avoid rapid expansions in the forward portion since the Newtonian concept will not account for strong overexpansion which could alter the flow at the inlet entrance.

Uniform Newtonian impact angle need not be imposed over the entire undersurface span since the spanwise control boundary is initially defined by the width of the engines, where the engine width is determined from

preliminary inlet capture requirements and the cowl or shock height. The surface geodesics define the spanwise boundary upstream of the inlet station (figure 5). However, note that the overall forebody planform is unrestricted. The assumptions used to establish the boundaries over which the surface must be tailored are quite adequate for bottom mounted engines, and variations of this technique could be expected to produce uniformly precompressed flows for sidemounted or displaced inlets. However, at lower Mach numbers (e.g. $M < 3$), a more sophisticated procedure such as linear theory may be required to determine the Mach lines which define the body surface and inlet cowl boundaries.

RESULTS AND DISCUSSION

This forebody design method has been applied to a hypersonic research airplane design study and the resulting flow fields were verified by three-dimensional characteristics calculations. The basic vehicle illustrated in figure 6 emphasized several advanced and promising new concepts for high performance airbreathing hypersonic aircraft. Fixed geometry scramjets were fully integrated with the vehicle airframe where the forebody was used to uniformly precompress the inlet flow and the entire afterbody was used as an exhaust nozzle. Structures, propulsion, aerodynamics and systems requirements were considered to produce a vehicle capable of systematically flight testing several of the most promising advanced concepts for hypersonic flight (ref. 11). The payloads and overall flight capability of this vehicle are beyond the scope of this paper; however, several features which affect the forebody design are presented here. This vehicle was to be air-launched and rocket accelerated to at least Mach 4. Scramjet acceleration and cruise capability

was required at all speeds between Mach 4 and 10. The scramjet engine employed was a hydrogen-fueled fixed-geometry modular concept which is currently under development at Langley (refs. 12,13). Identical modules were imposed as a ground rule in the research airplane design study to minimize the complexity and cost of the research scramjet propulsion system. The vehicle forebody geometry was tightly constrained by the large forward volume requirements in the payload bay to accommodate the hydrogen fuel tank, and the size limitations imposed by the carrier vehicle (B-52).

Some of the potential performance payoffs which can be achieved through forebody design, are illustrated through the key constraints and flow requirements imposed in this design study. The volume of the forebody is generally determined without considering the inlet flow conditions and is primarily a function of the internal system requirements, center of gravity control, and vehicle aerodynamics. A perspective of the volume requirements imposed in this study is indicated in figure 7 where the cross-sectional area and radius of an equivalent axisymmetric body for the design vehicle are presented as a function of distance from the nose. The distributions for a cone and an ogive cylinder are shown for comparison. The length of the cylinder on the ogive cylinder was determined from equation (16) using the initial cowl height and center-line precompression requirements for the research airplane concept. The cone which gives the closest approximation to the planform and profile limitations of the vehicle has a 5° half angle. These three bodies form a boundary of potential axisymmetric forebody designs.

Mach 10 Forebody Flows

If we consider the flow field about the three bounding forebodies (figure 7) at flight conditions corresponding approximately to Mach 10 cruise,

it is apparent from figure 8 that the flow at the inlet entrance is not uniform. The angle of attack of each body was determined such that the local angle between the lower center-line and the wind vector was 10 degrees at the inlet entrance. The local Mach number, pressure ratio, and relative mass flow are presented near the body surface and at a specified cowl height as a function of percent body semispan. These data were obtained from the three-dimensional characteristics program of reference 7. Each of these bodies exhibits a strong spanwise variation in each of the flow parameters, and except for the cone there is a significant variation between body and cowl lip at each spanwise location.

The detrimental effect that such flows can have on engine performance can be readily seen by examining the variation in relative mass flow across the vehicle span. For the vehicle displayed in figure 6, the mass flow requirements to meet mission goals were initially based on design center-line (surface plane of symmetry) values and engine installation across 80 percent of the body semispan. An examination of the average mass flow across the span of these three bodies, as illustrated in figure 8, indicates a 25 percent drop-off from the center-line design value to the most outboard position (80 percent semispan), and a corresponding engine performance potential roughly 25 percent less than the initial design value.

This is not an exact representation of performance potential because the shock standoff distance increases from the center-line out across the span and more inlet capture could be utilized if nonsimilar modules were employed. However, as stated earlier, identical engine modules was a ground rule for this study.

The forebody design procedure based on Newtonian impact angle was used to create a geometry within the forebody volume constraints of the research airplane. The spanwise area of interest included 80 percent of the semispan and the upstream boundary was determined from Mach 10 cruise conditions. Maximum effective inlet capture becomes increasingly important with increasing Mach number and therefore the bow shock was taken as the vertical boundary at the inlet face. The flow at the inlet face from this forebody design is superimposed (figure 9) on the previous results for the axisymmetric equivalent (based on cross-sectional area distribution) to the research airplane forebody. The cross-hatched regions denote the axisymmetric forebody results of figure 8b. Both the spanwise and vertical variations in all parameters are markedly decreased; however, the most graphic improvement occurs in the available mass flow across the 80 percent semispan of interest. The average center-line value of mass flow for the tailored forebody is increased by approximately 25 percent over that of the axisymmetric equivalent even though the local surface center-line inclination at the inlet entrance is 10° for both forebodies. The integrated average mass flow across 80 percent of the semispan of the tailored forebody is approximately 33.5 percent higher than that of the axisymmetric equivalent. The angle of attack of the axisymmetric equivalent could be increased until the average center-line values of mass flow were equal on the two forebodies; however, the integrated average mass flow on the tailored forebody would still be approximately 7 percent larger than the axisymmetric equivalent. This difference will be amplified by the increased flow nonuniformity that is bound to occur on the axisymmetric forebody as the angle of attack is increased. These comparative advantages of tailored forebodies are signifi-

cant; however, a more objective evaluation of the design technique can be made by analyzing inlet entrance flows in light of the forebody design goals listed on figure 3.

Several alternate designs were generated during this study and additional flow parameters such as shock stand-off distance and flow angularity were examined to assess their relationship to the forebody-inlet interaction. Three forebodies with variations in fineness ratio (volume) and cross-sectional shape are shown in figure 10. As stated earlier, the forebodies presented in this paper are constructed from bielliptic cross-sections so that the flow fields could be verified with three-dimensional characteristics calculations using the method of reference 7. The major to minor axis ratios for the lower surfaces of forebodies 1, 2, and 3 are 7, 3.5, and 2, respectively. The spanwise control boundary for each of these bodies was at 80 percent of the body semispan. The design angle of attack was 10° relative to the lower surface center line and the boundary height perpendicular to the surface was taken as the shock height at the Mach 10 and $\alpha = 10°$ flight conditions. The body listed as forebody 1 is the same forebody presented in figure 9. The flow conditions at the inlet face (control area) which are generated by these forebodies are shown in figure 11. The spanwise variations of each parameter are small as are the variations from body to cowl lip (or bow shock). The magnitudes of these variations will be discussed more fully later in the paper. The main point illustrated in figure 11 is the close similarity between these flows even though the fineness ratios and cross-sectional shapes are quite different (e.g. the average local cross-sectional curvature of forebody 3 is approximately twice that of forebody 1).

A more complete representation of the flow at the inlet face is illustrated by inlet station isograms in figures 12 through 14. These isograms clearly indicate the variations in pressure, local Mach number, flow sidewash angle relative mass flow, as well as the shock stand-off distances. The lateral bound of the control area is indicated in each figure by a dashed line normal to the surface. The maximum pressure deviation over the control area for all three bodies is less than 10 percent. The local values and gradients are similar for each of the three forebodies. The maximum Mach number deviation is 5 percent or less. The predominant flow parameter is mass flow which changes in distribution for these forebodies from a slightly vertically striated flow for forebody design 1 to a slightly spanwise striated flow for forebody design 3. The maximum spanwise deviation is less than 4 percent for each forebody. The maximum overall deviation in mass flow is 10 percent, which occurs between body and shock for forebody 1.

The deviation in sidewash flow angle over the control area could affect inlet performance and the maximum deviation is 4.5° which occurs on forebody 3 as expected because of its increased cross-sectional curvature. However, the effect of this flow angularity can be reduced to acceptable levels without additional forebody tailoring because of the modular design of the scramjet. Five engine modules were used across the total span and if each module is aligned with the average direction of the flow being captured, then the maximum flow angularity experienced by any one module is less than $\pm 1°$. However, a small external cowl drag penalty is incurred when the modules are canted inboard. Thus, the optimum orientation of the engine modules must be determined through trade-offs between cowl drag and inlet performance.

Maximum effective inlet capture is also a forebody design goal and

occurs when the forebody bow shock is coincident with the cowl lip for the integration concept in this study. Uniformity of shock stand-off distance is the primary criterion of merit in achieving this goal within the identical engine module constraint. For these bodies there is a slight decrease in shock stand-off distance across the body semispan with the minimum height occurring at the outboard control area boundary. All three forebodies provided approximately 90 percent effective capture of the available precompressed flow when constrained to the largest constant height inlets that could be accommodated between the body and bow shock.

For the three forebody designs illustrated in figures 12 through 14, the shock stand-off distance at the design Mach number and angle of attack was approximately equal to one-half the body semispan. Therefore, forebody 1 will have higher drag due to its lower fineness ratio and the final choice will be a trade-off between aerodynamic and inlet capture efficiencies. In this study the volume constraint tended to drive the optimum choice toward forebody 1. The nearly linear variation of shock stand-off distance with forebody semispan for these bodies also allows rapid estimates of inlet capture efficiency within moderate changes in longitudinal engine location, which is a key parameter in nozzle integration (ref. 6).

Off-Design Forebody Flows

The inlet entrance flow at off-design flight conditions resulting from tailored forebodies also plays an important role in the overall measure of forebody effectiveness since the vehicle must perform efficiently at Mach numbers and angles of attack other than those encountered at cruise. The scramjet acceleration portions of the flight envelope of this vehicle resulted in approximate forebody angles of attack of 6° across the Mach number range.

The primary flow parameters, local Mach number, pressure, and relative mass flow for the three forebodies are presented in figure 15 as functions of percent body semispan for Mach 10 accelerations.

Again, the relative mass flow is a key parameter in determining forebody effectiveness. The average mass flow for each forebody design was reduced because of the lower angle of attack; therefore, the real criteria of merit are the vertical and spanwise mass flow variations across the inlet face. A slight positive spanwise gradient occurs at Mach 10 at the 6° acceleration angle of attack. This is most noticeable in the surface values for forebody 1; however, the maximum spanwise variation for each forebody occurs near the 80 percent semispan location and deviates less than 6 percent from the center-line value. These gradients are slightly positive in contrast to the large negative gradients shown for the axisymmetric bodies in figure 8. The slight positive gradients could be beneficial if an increase in fuel scheduling complexity were acceptable. The vertical gradients in mass flow are almost identical with those shown in figure 11 for the cruise conditions and are within the design goals.

The variations in inlet flow conditions with flight Mach number are shown for forebody 1 in figure 16. The same three flow parameters are again presented as the basic measure of merit for Mach numbers 4, 6, and 8 at acceleration angles of attack. At the lower Mach number, a negative spanwise gradient in both pressure and relative mass flow occurs slightly inboard of the 80 percent semispan control boundary. However, the spanwise gradients shown in figure 16 from Mach 4 to Mach 8 are less than the vertical gradient in mass flow for forebody 1 at cruise design conditions. The magnitudes of these off-design variations are within the initial forebody design goals.

FUTURE STUDY AREAS

The results of this study represent a first step in developing the technology base necessary to efficiently integrate scramjets with the vehicle airframe by identifying some major trends resulting from forebody-inlet-airframe interactions. However, much remains to be done before optimum integration can realistically be achieved. Listed below are some forebody-inlet items which are amenable to state-of-the-art analytic techniques and are currently under investigation.

(1) The effects of boundary-layer displacement and other viscous effects must be included in the forebody tailoring scheme.

(2) The effect of vehicle yaw on forebody flow fields must be assessed.

(3) Forebodies employing hard chines at maximum span should permit the highest percent span utilization and should be included in analytic capability.

(4) At lower Mach numbers, more exact techniques for determining the forebody influence boundaries must be applied for sidemounted inlets or inlets which are significantly displaced from the vehicle surface.

CONCLUDING REMARKS

The geometric shape of forebodies on highly integrated hypersonic vehicles has a significant effect on the overall vehicle performance. When the flow at the inlet entrance has been uniformly precompressed, the engine size, weight, and drag can be more easily minimized. In addition, uniform flow has a beneficial effect on the required complexities in inlet design and fuel scheduling between engine modules.

A forebody design procedure has been developed to generate surfaces which produce nearly uniform flows at the entrance of bottom mounted inlets. The procedure has been verified in a vehicle design study where several forebodies were generated which exhibited minimum variations in key flow parameters both across the vehicle span and across the shock layer. The bow shock stand-off distance is also rendered nearly uniform so that at hypersonic cruise conditions a near-maximum effective inlet capture schedule can be achieved. Flow angularities were examined, and although they were not nulled, they were found to be of acceptable levels (less than $\pm 1°$ across any single engine module employed in the design study). The basic nature of the forebody flow is maintained across the normal scramjet portion of the design vehicle flight envelope which included a Mach number range from 4 to 10 and angles of attack from 6° to 10°.

These studies indicate that good inlet flow can be achieved by tailoring only the portion of the vehicle surface which has direct influence upon the inlet capture area. Therefore, reasonable geometries can be generated to meet constraints which are imposed by other disciplines such as aerodynamics, structures, and internal systems.

REFERENCES

1. Becker, John V., and Kirkham, Frank S.: Hypersonic Transports. NASA SP-292, Paper No. 25, Nov. 1971, pp 429-445.

2. Nagel, Adelbert L. and Becker, J. V.: Key Technology for Airbreathing Hypersonic Aircraft. Presented at the AIAA 9th Annual Meeting and Technical Display, Washington, D.C., Jan. 8-10, 1973.

3. Becker, J. V.: New Approaches to Hypersonic Aircraft. Seventh Congress of the International Council of the Aeronautical Sciences, Rome, Italy, Sept. 14-18, 1970.

4. Small, William J., Fetterman, David E., and Bonner, Tom F. Jr.: Alternate Fuels for Transportation. Part 1: Hydrogen for Aircraft. Mechanical Engineering, May 1974, pp 18-24.

5. Gregory, T. J., Williams, L. J., and Wilcox, D. E.: The Airbreathing Launch Vehicle for Earth Orbit Shuttle - Performance and Operation. Presented at AIAA Advanced Space Transportation Meeting, Feb. 4-6, 1970.

6. Small, W. J., Weidner, J. P. and Johnston, P. J.: Scramjet Nozzle Design as Applied to a Highly Integrated Hypersonic Research Airplane. NASA TM X-71972, 1974.

7. Chu, C. W., and Powers, S. A.: The Calculation of Three-Dimensional Supersonic Flows Around Spherically-Capped Smooth Bodies and Wings. Technical Report AFFDL-TR-72-91, Vols. 1 and 2, Air Force Flight Dynamics Laboratory, Wright-Patterson AFB, Ohio, Sept. 1972.

8. Gunness, R. C. Jr., Knight, C. J., and D'Sylva, E.: Flow Field Analysis of Aircraft Configurations Using a Numerical Solution to the Three-Dimensional Unified Supersonic/Hypersonic Small Disturbance Equations, Part I. NASA CR-1926, Feb. 1972.

9. Rakich, J. V.: Application of Three-Dimensional Method of Characteristics to Noncircular Bodies at Angle of Attack. NASA SP-228, Paper No. 9, Oct. 1969, pp 159-176.

10. Kutler, P., and Lomax, H.: A Systematic Development of the Supersonic Flow Fields Over and Behind Wings and Wing-Body Configurations Using a Shock Capturing Finite Difference Approach. AIAA Paper No. 71-99, AIAA 9th Aerospace Sciences Meeting, New York, New York, Jan. 25-27, 1971.

11. Kirkham, F. S.,and Driver, C.: Liquid Hydrogen Fueled Aircraft -- Prospects and Design Issues. AIAA Paper No. 73-809, presented at the AIAA 5th Annual Aircraft Design, Flight Test, and Operations Meeting, St. Louis, Missouri, Aug. 6-8, 1973.

12. Anderson, G. Y.: An Examination of Injector/Combustor Design Effects on Scramjet Performance. Presented at the 2nd International Symposium on Air Breathing Engines, Sheffield, England, March 25-29, 1974.

13. Henry, J. R.,and Anderson, G. Y.: Design Considerations for the Airframe-Integrated Scramjet. NASA TM X-2895, December 1973.

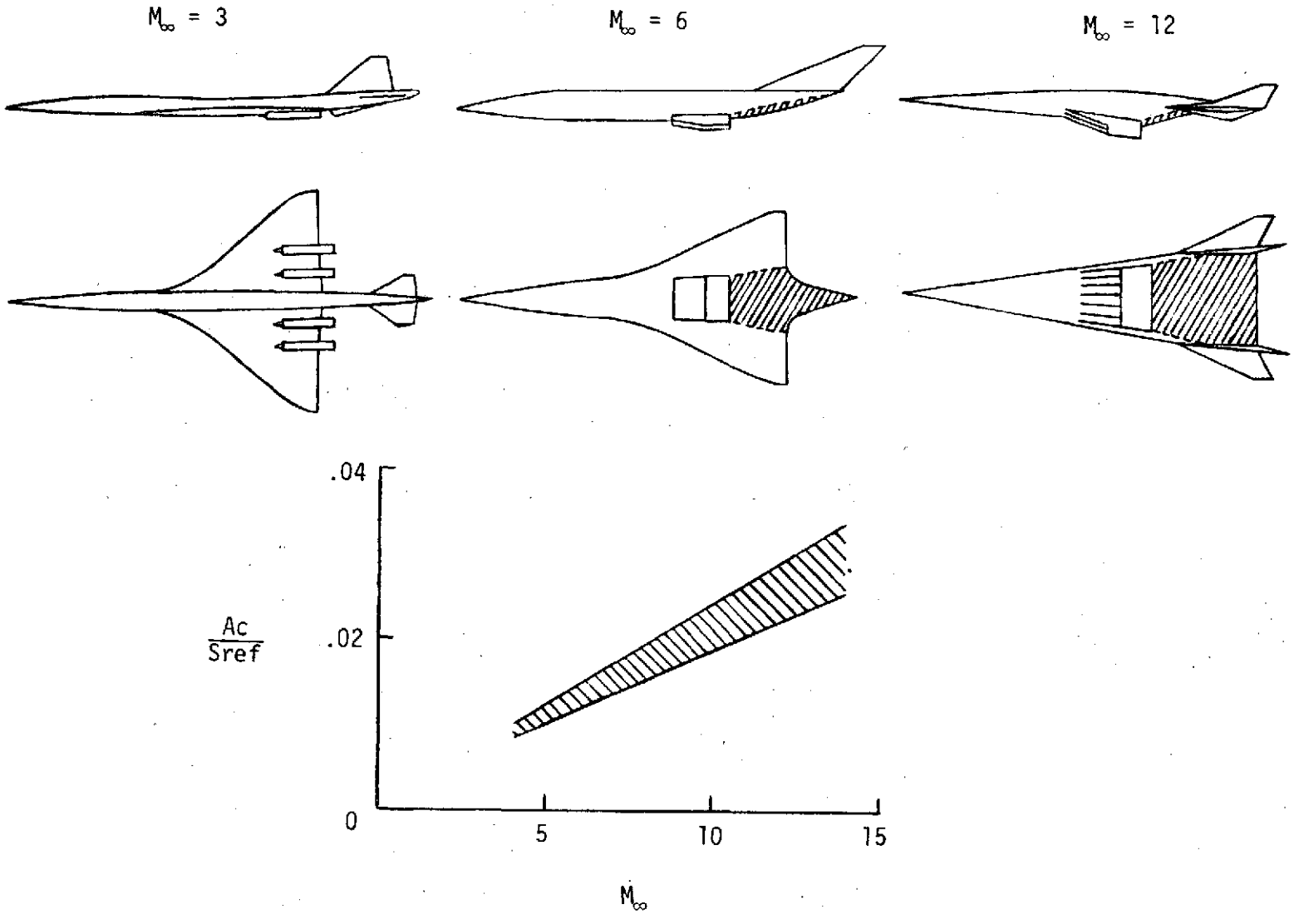

Figure 1.- Required inlet capture.

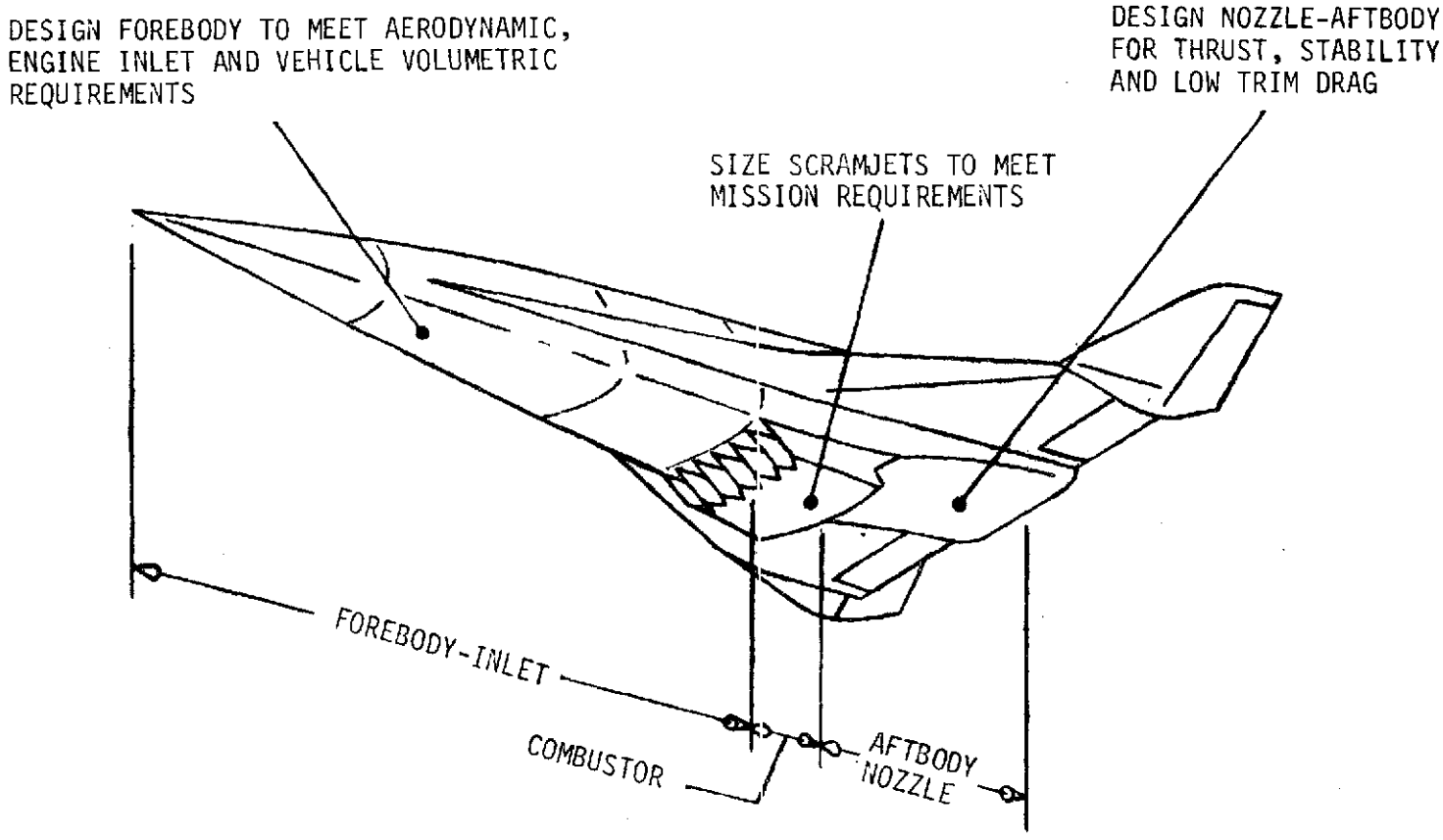

Figure 2.- Design features for efficient engine airframe integration

DESIGN GOALS

- MINIMIZE INLET FLOW GRADIENTS
  - MASS FLOW
  - PRESSURE
  - LOCAL MACH NUMBER
- MINIMIZE SENSITIVITY WITH MACH NUMBER AND ANGLE-OF-ATTACK
- MAXIMIZE EFFECTIVE INLET CAPTURE
- MAINTAIN UNIFORM BOW SHOCK STAND-OFF DISTANCE

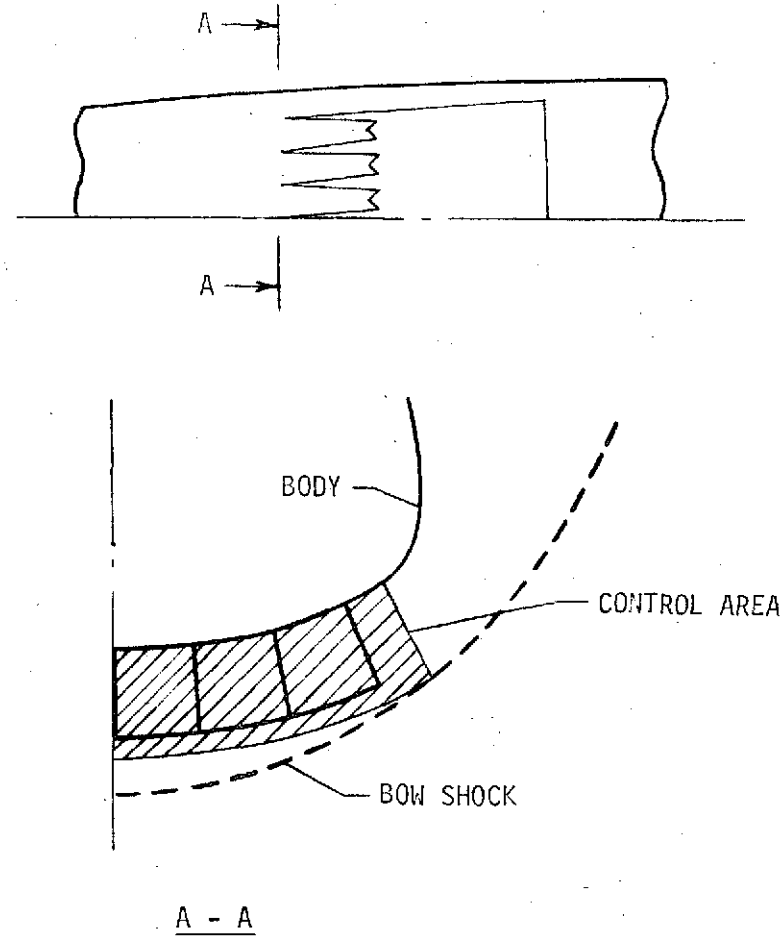

Figure 3.- Forebody design goals.

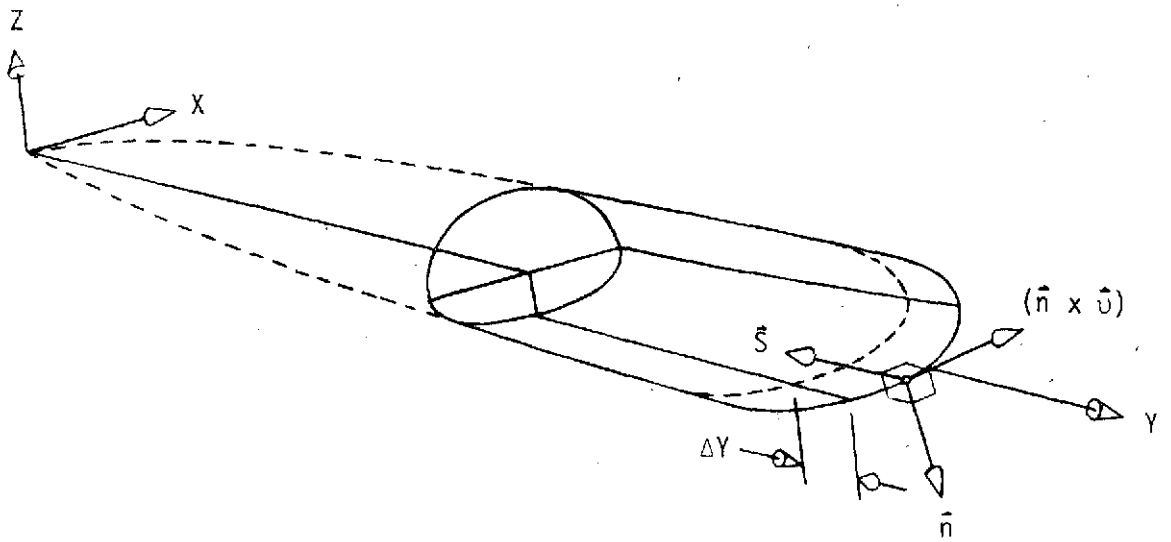

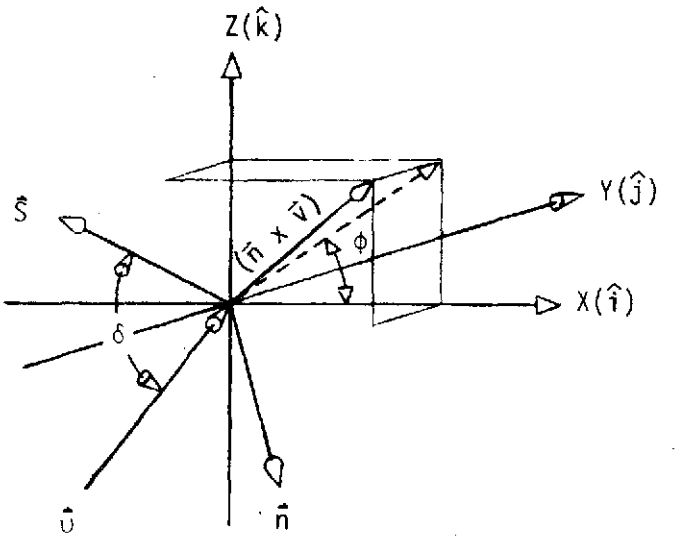

SKETCH OF LOCAL
VECTOR DIRECTIONS

Figure 4.- Relation between body geometry and wind vector for Newtonian impact angle.

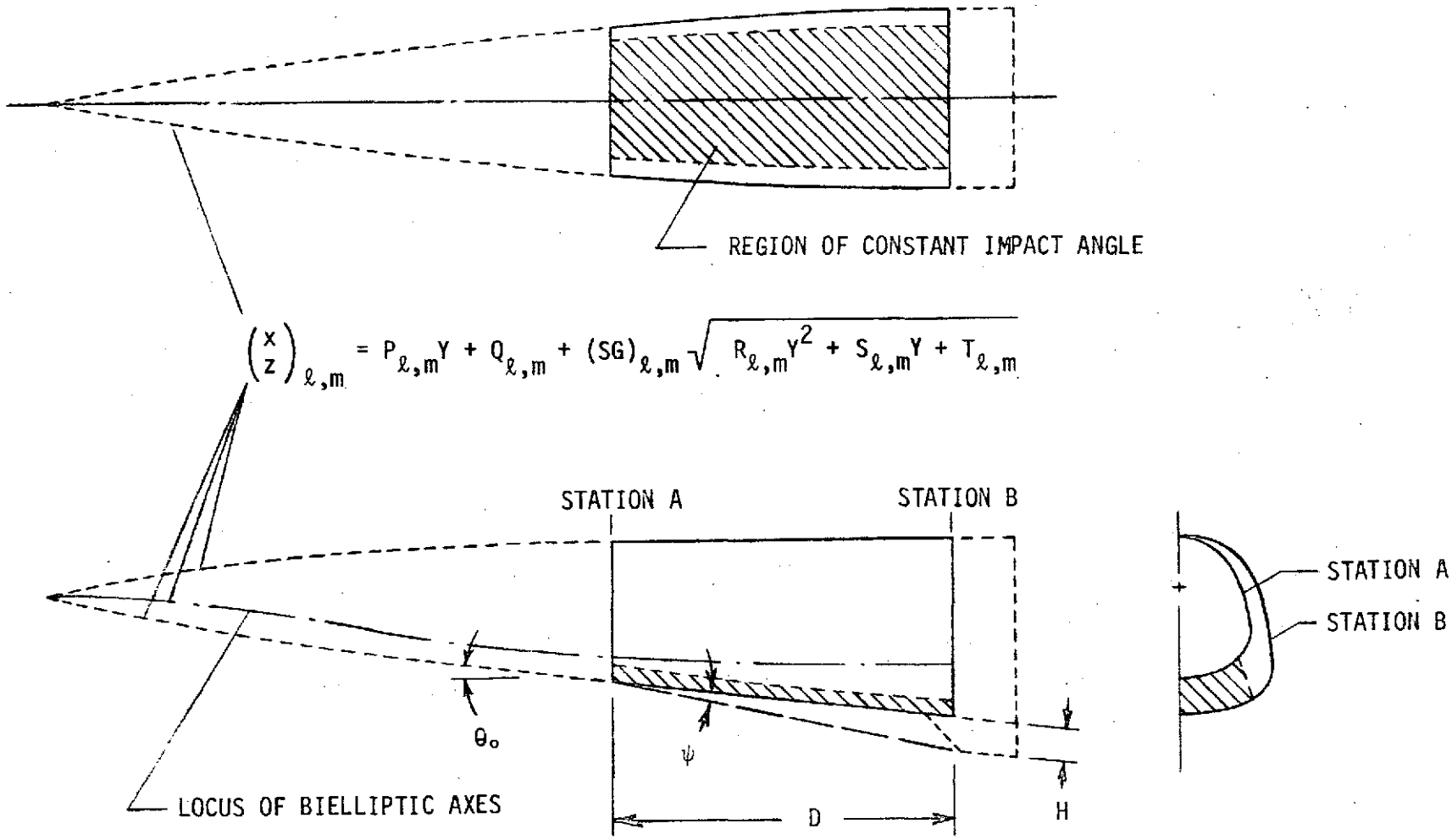

Figure 5.- Geometry definition for bielliptic forebody design

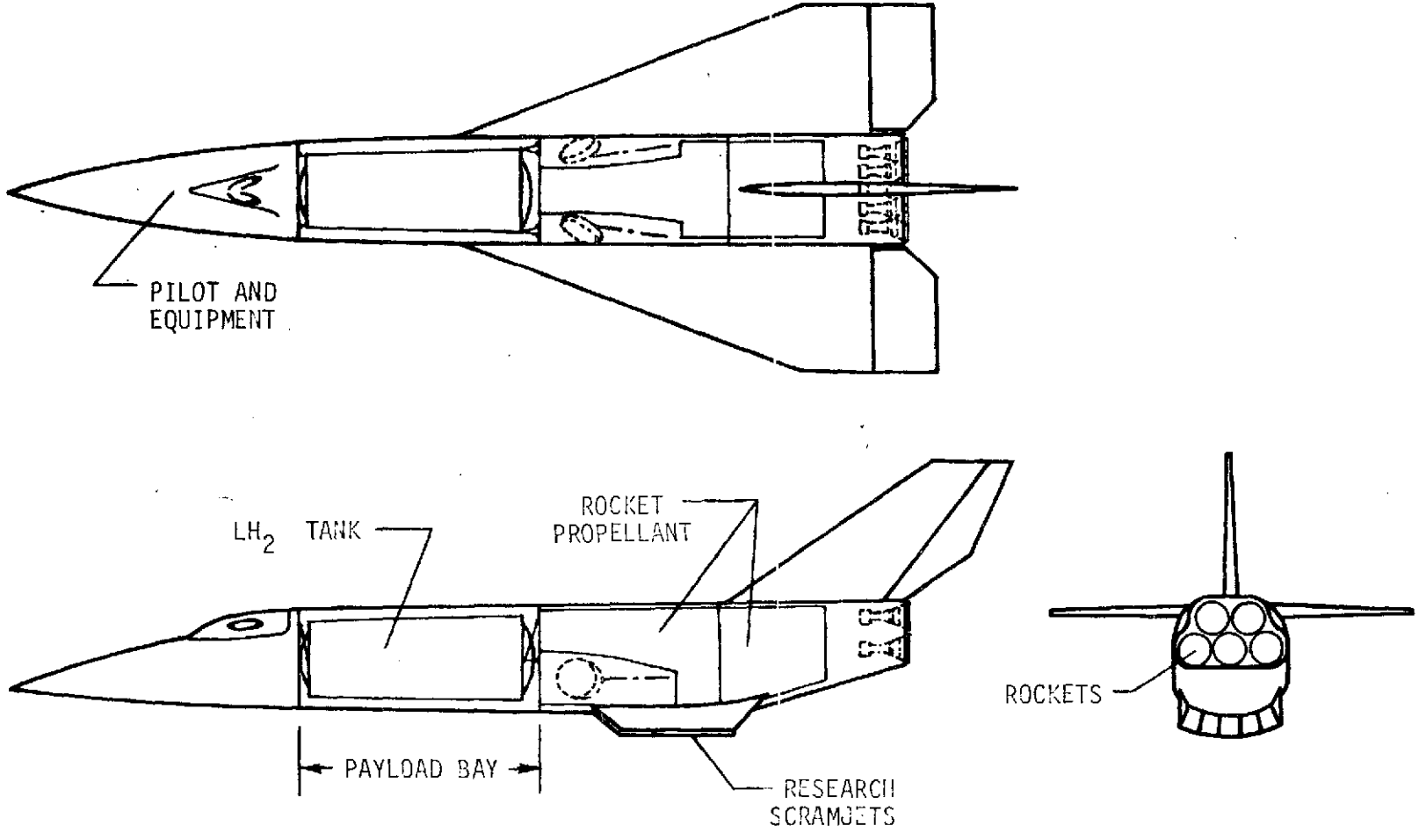

Figure 6.- Basic elements of high speed research airplane (HSRA)

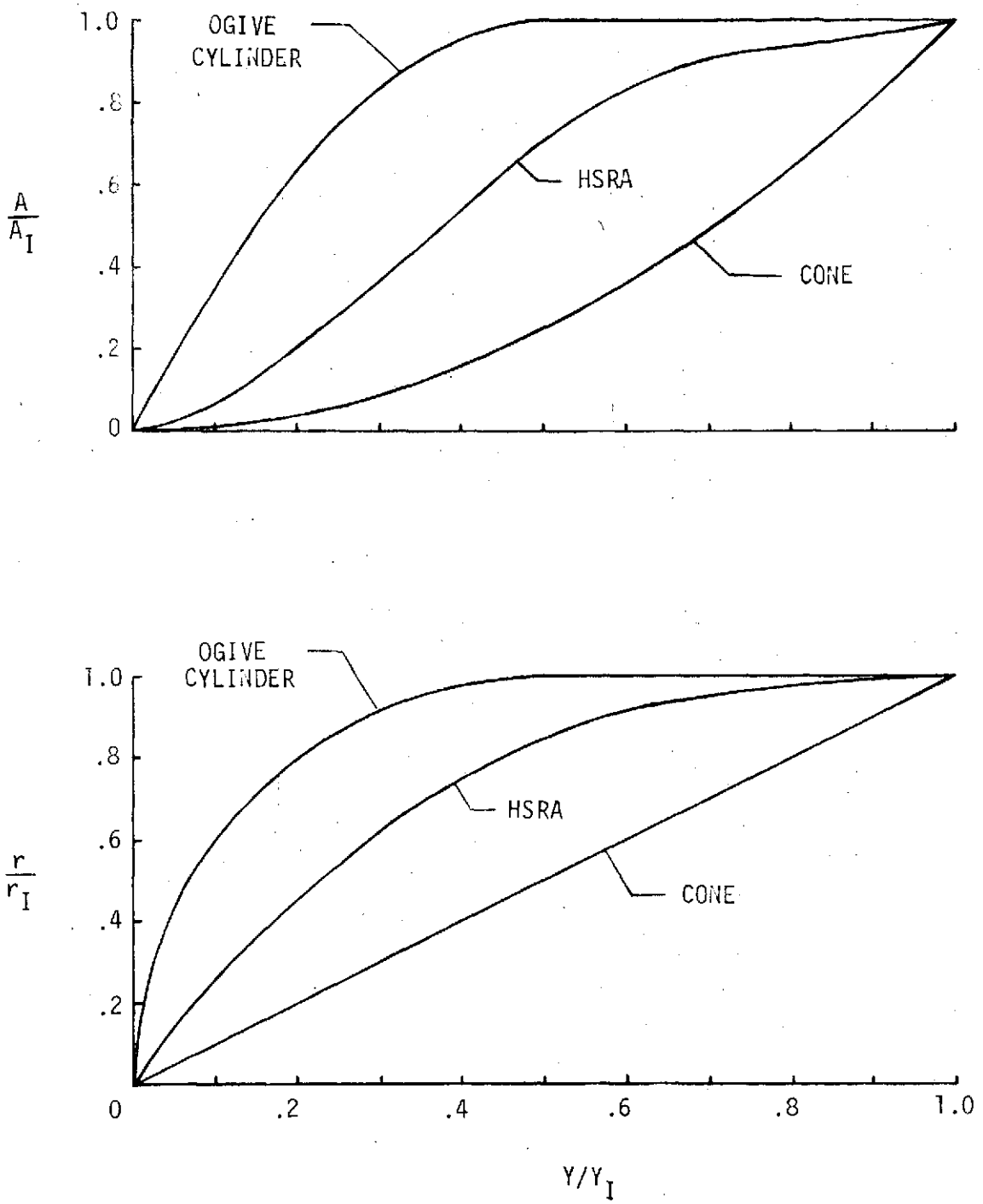

Figure 7.- Volumetric requirements of the high speed research airplane (HSRA) forebody

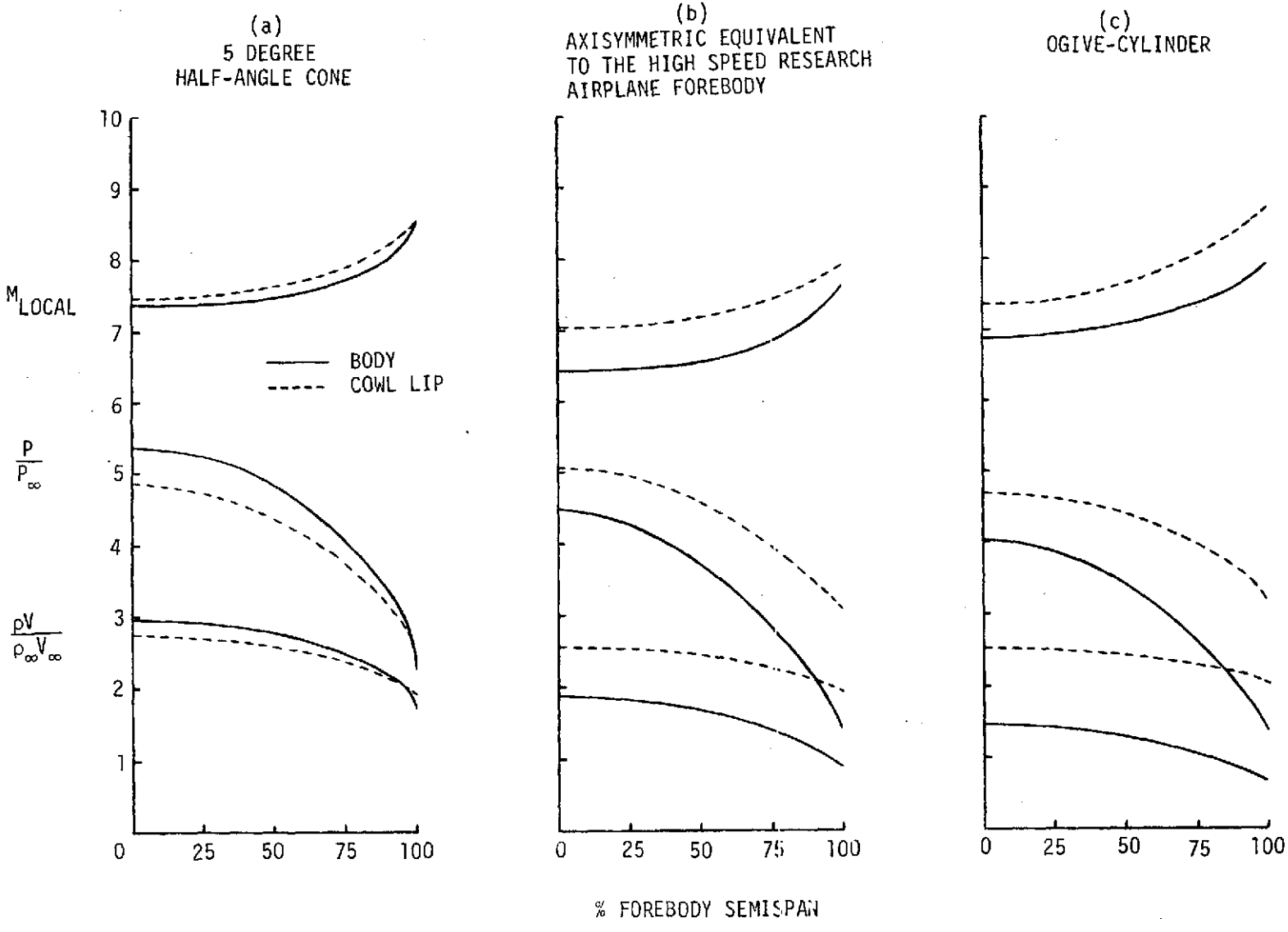

Figure 8.- Comparison of flow at the inlet entrance generated by axisymmetric alternatives to the High Speed Research Airplane forebody, $M_\infty = 10$, $\alpha = 10°$

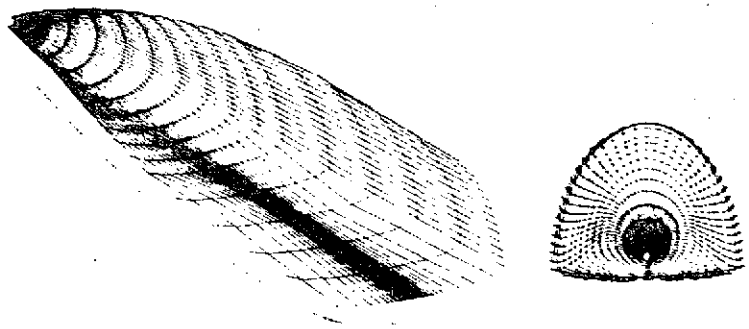

HIGH SPEED RESEARCH AIRPLANE FOREBODY DESIGN

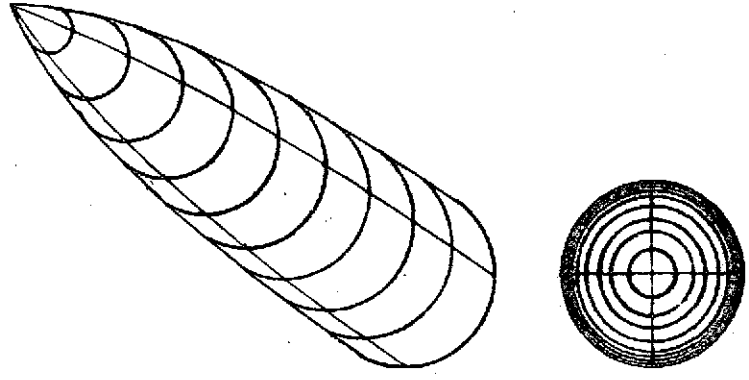

AXISYMMETRIC EQUIVALENT

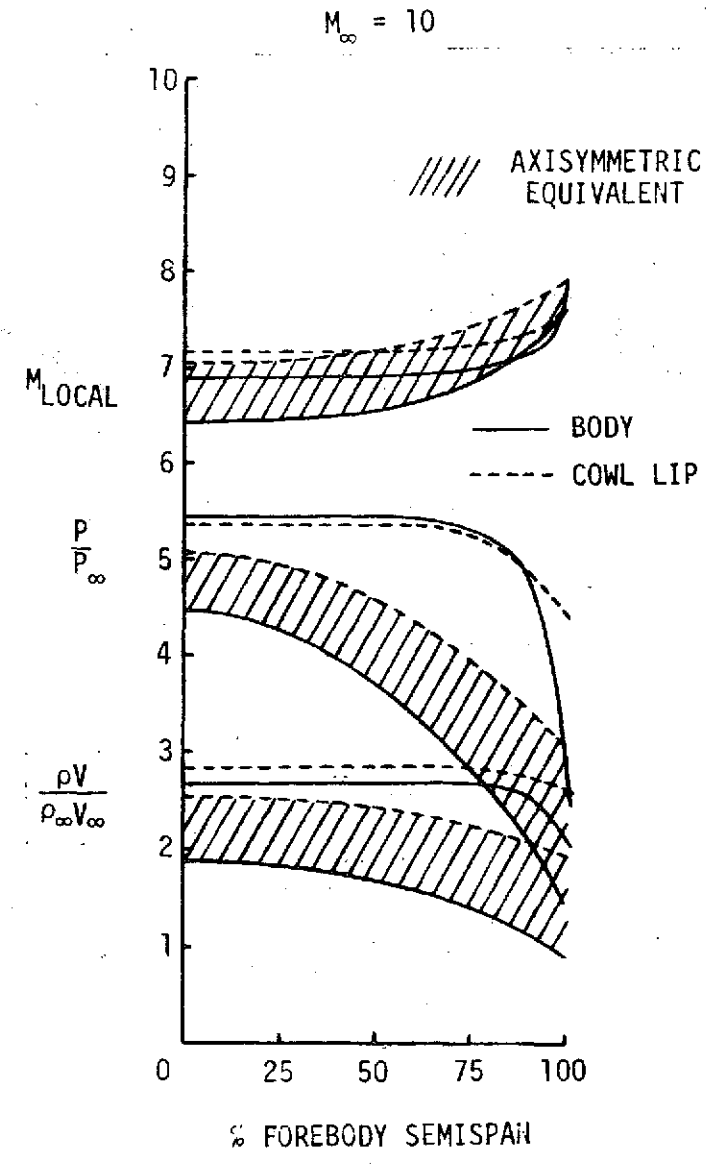

Figure 9.- Comparison of inlet entrance flow conditions between constant Newtonian impact angle forebody and its axisymmetric equivalent.

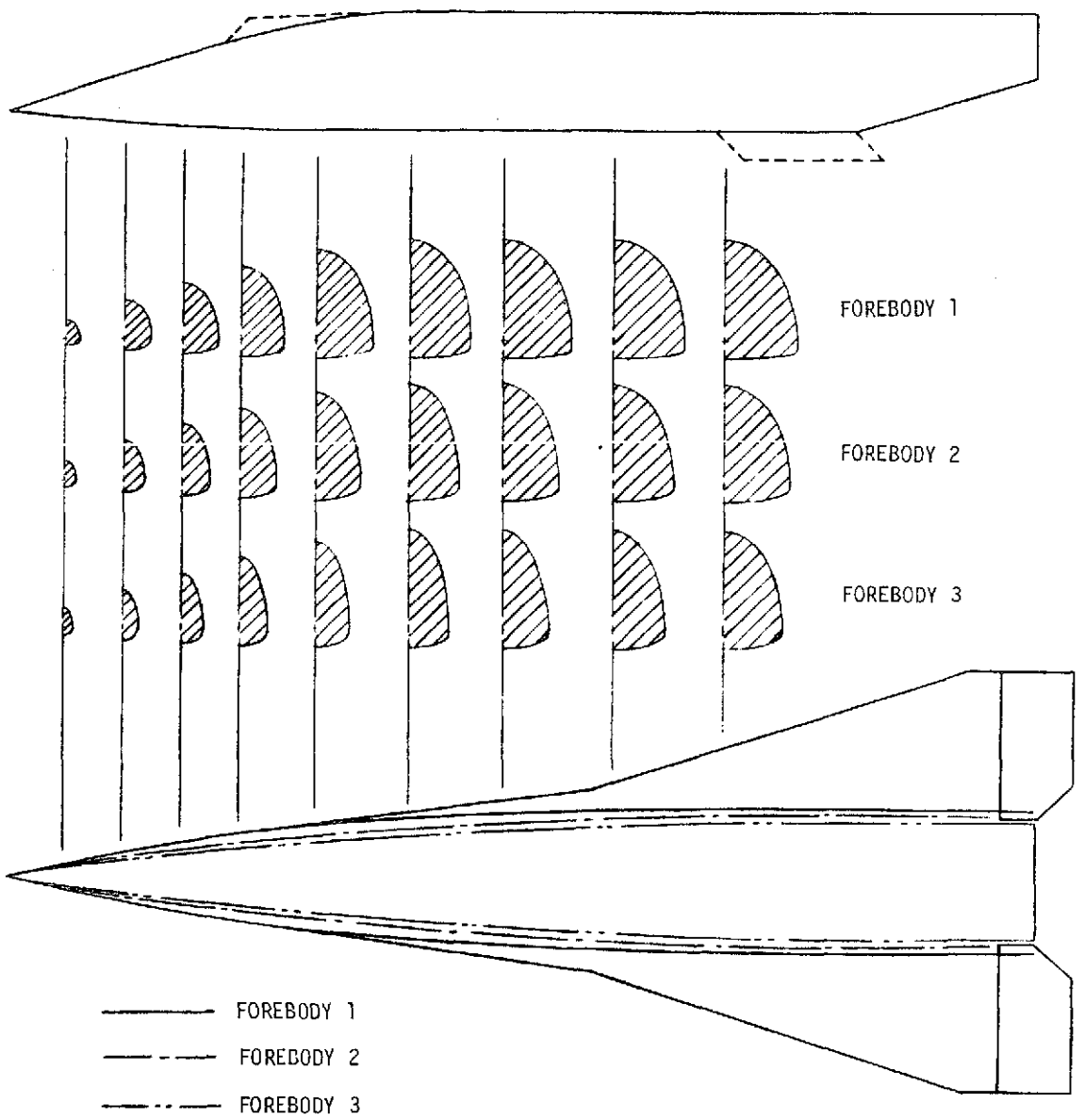

Figure 10.- Forebody designs producing uniform precompressed flow at the inlet entrance.

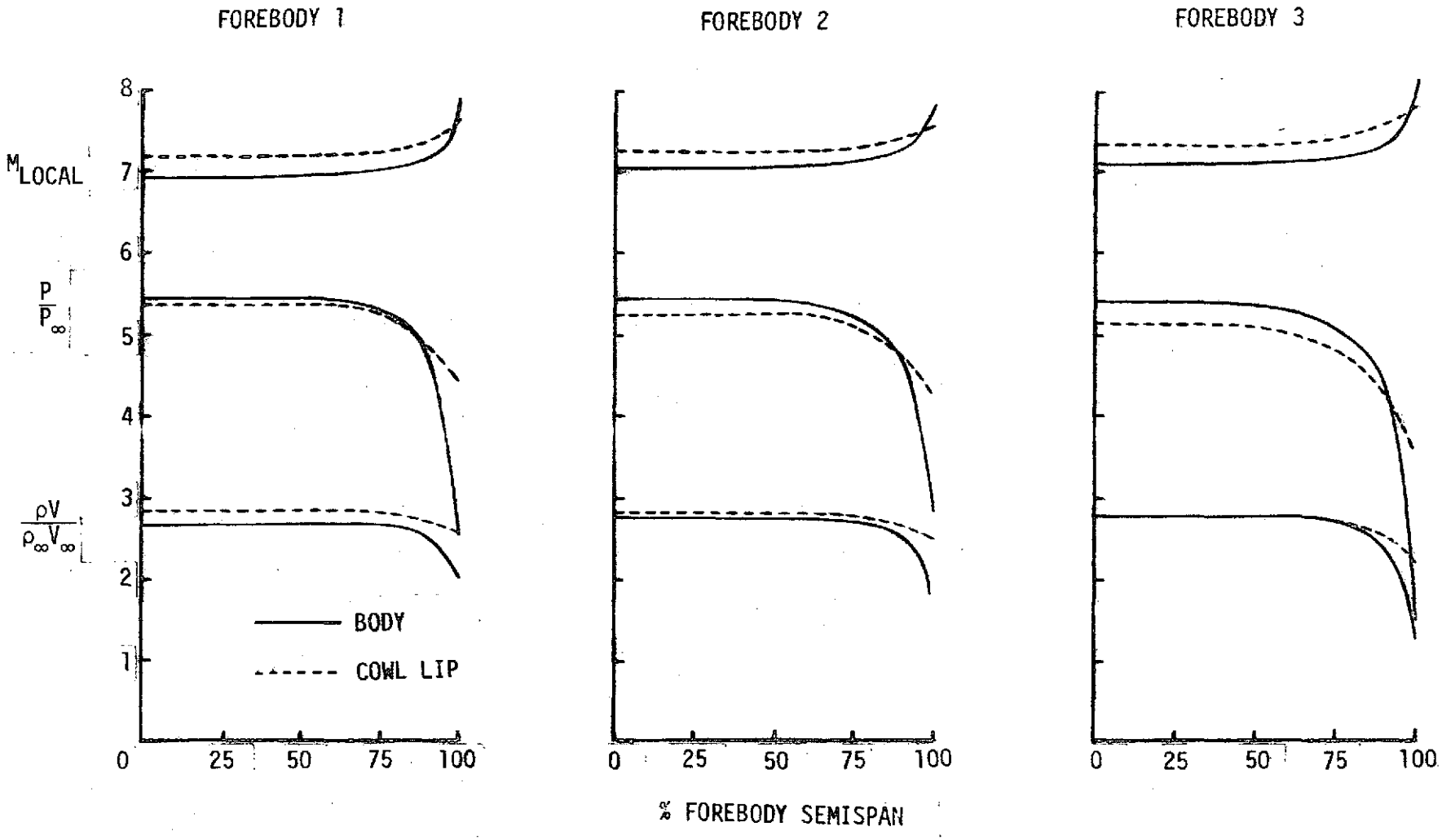

Figure 11.- Flow conditions at the inlet for three forebody designs at Mach 10 with 10° of precompression

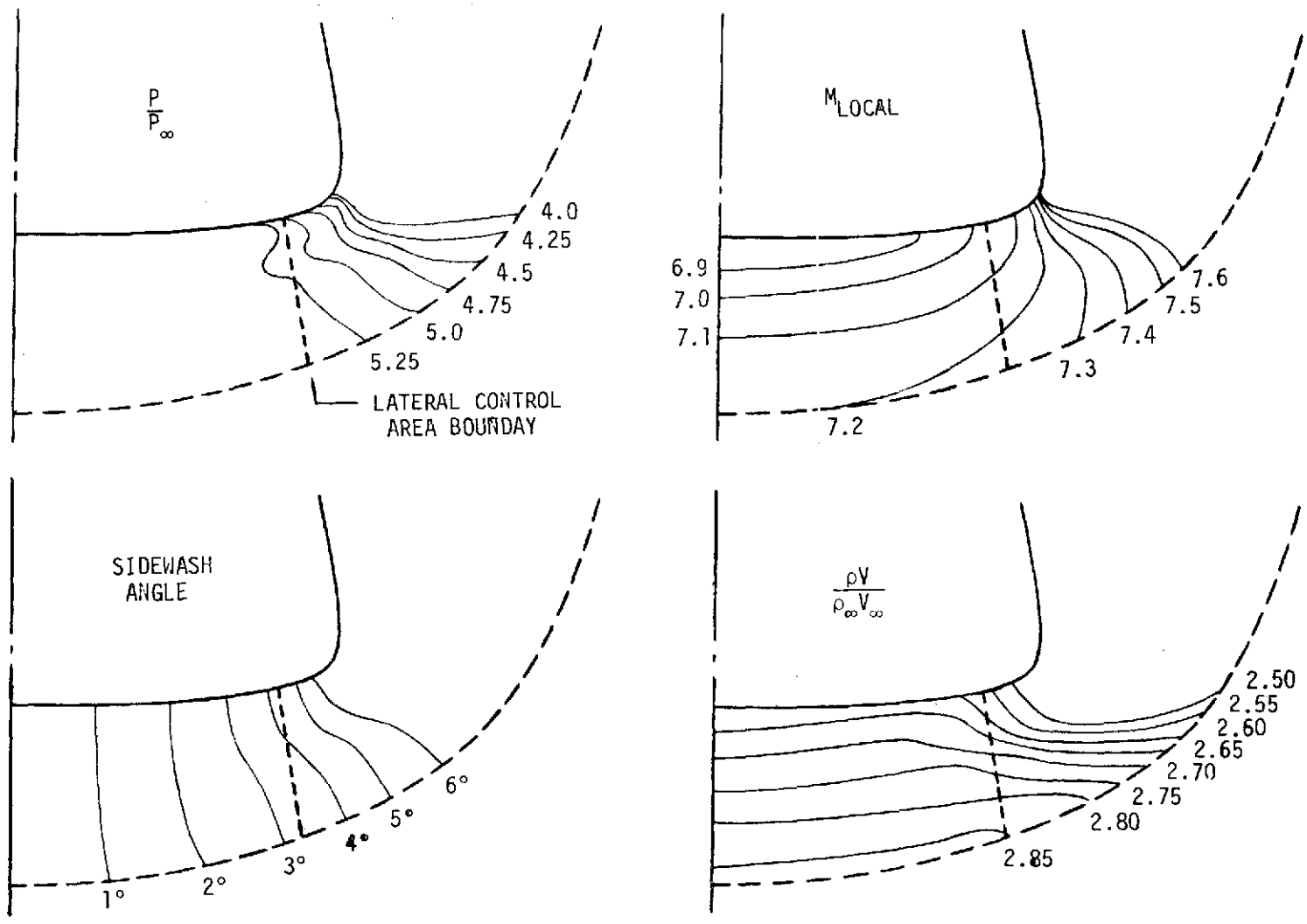

Figure 12.- Flow isograms at the inlet entrance produced by forebody 1 at Mach 10 and α = 10°

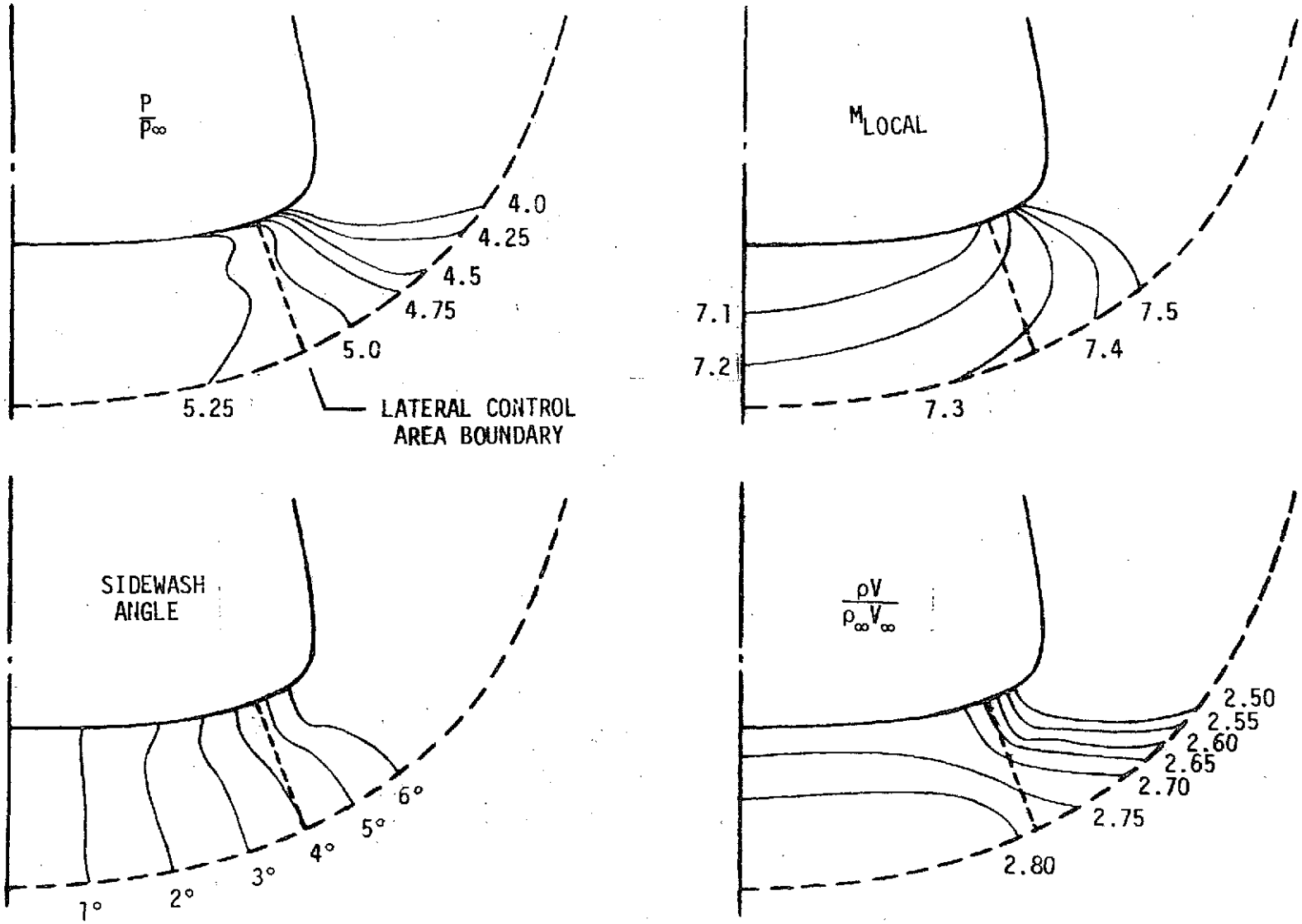

Figure 13.- Flow isograms at the inlet entrance produced by forebody 2 at Mach 10 and α = 10°.

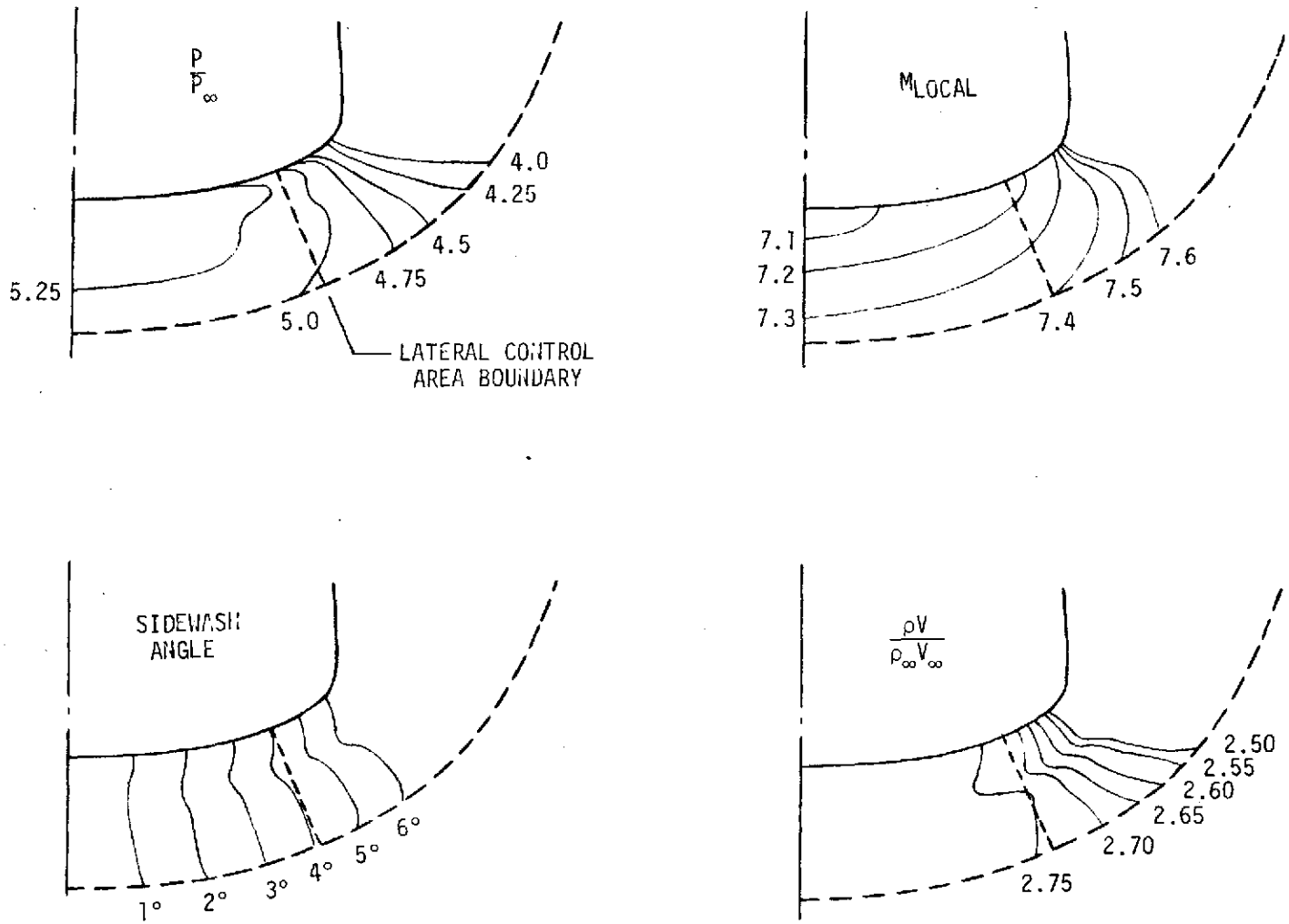

Figure 14.- Flow isograms at the inlet entrance produced by forebody 3 at Mach 10 and $\alpha = 10°$

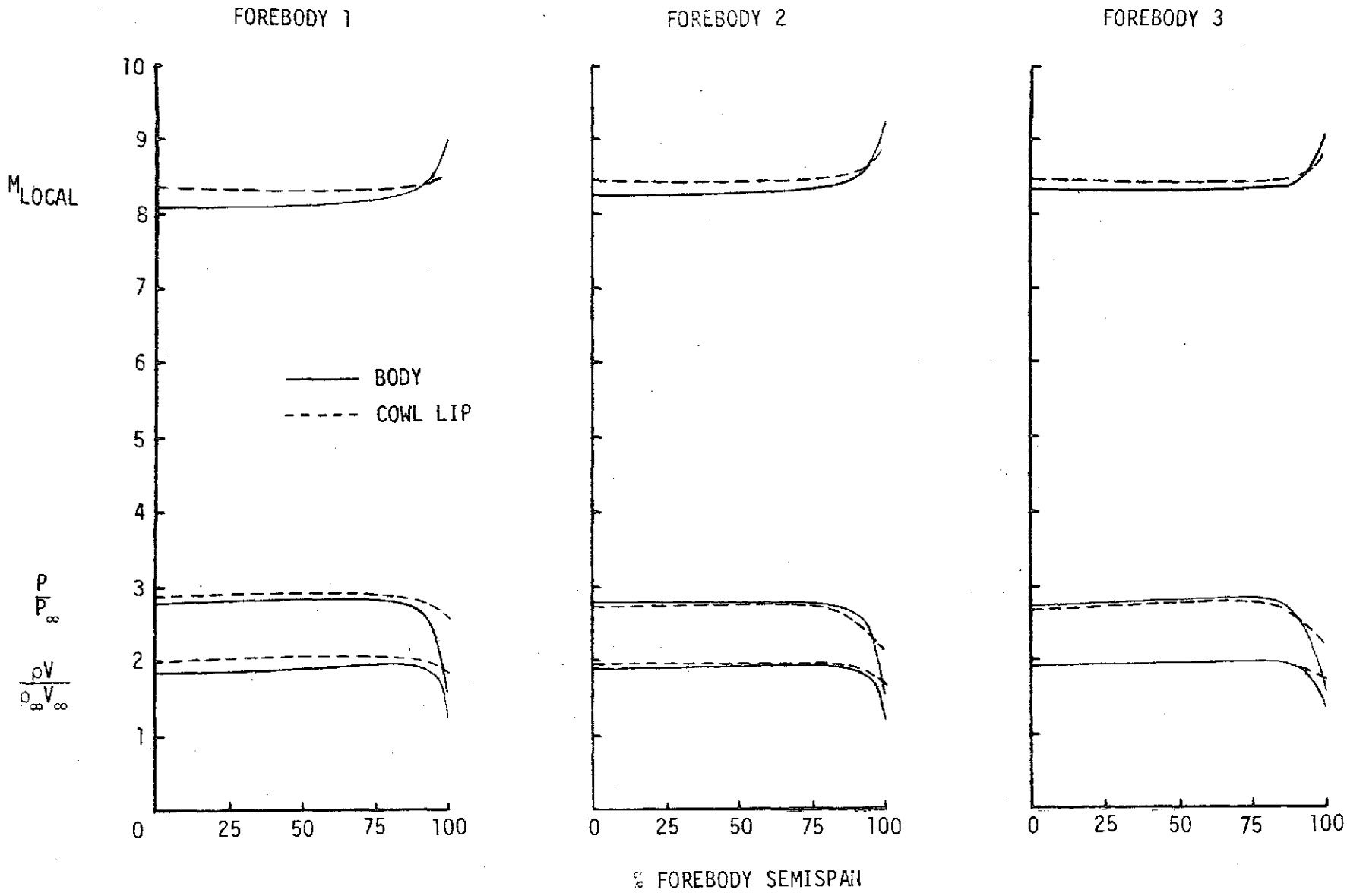

Figure 15.- Inlet entrance flow conditions corresponding to acceleration angle-of-attack (α=6°) at Mach 10.

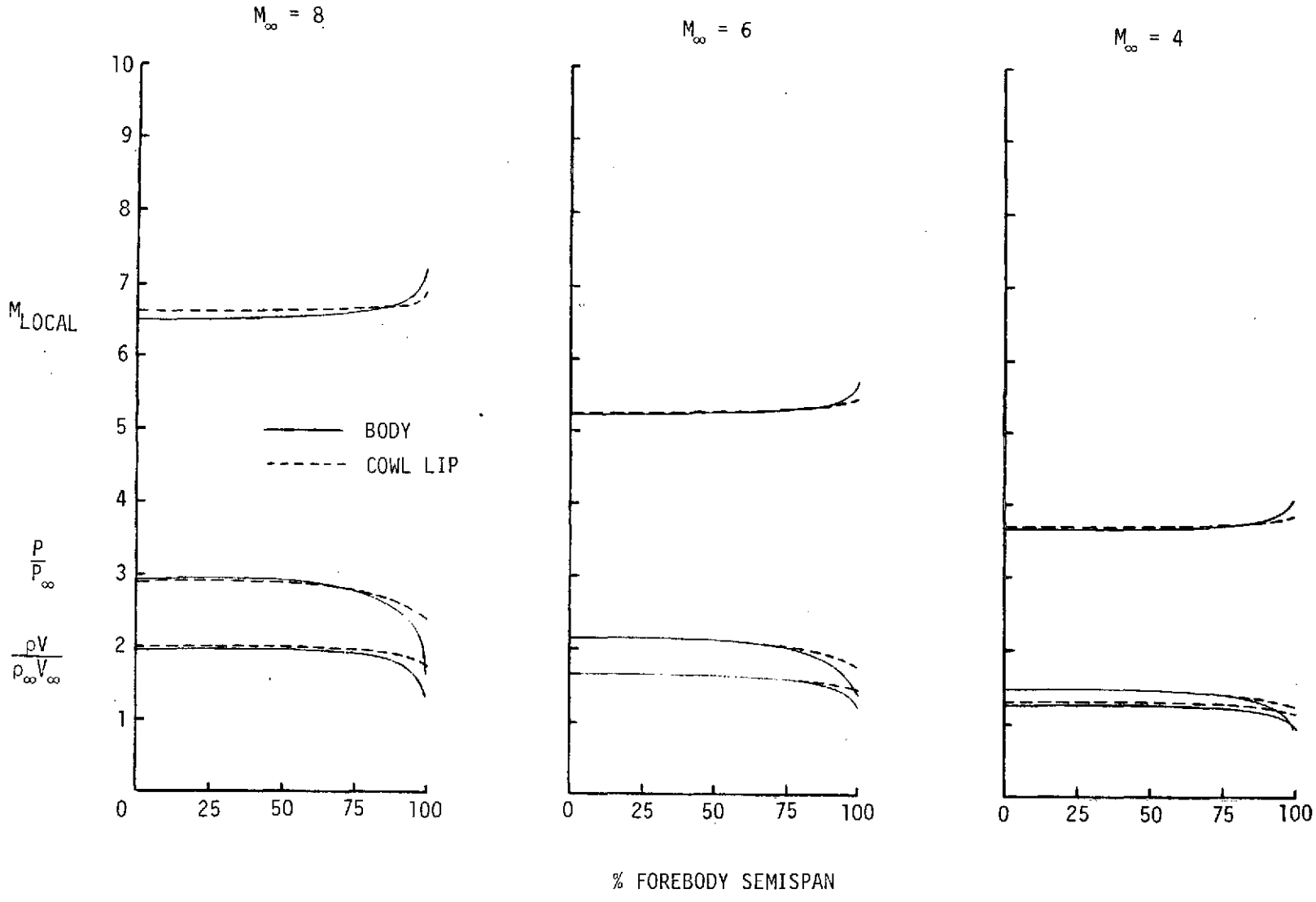

Figure 16.- Off-design flow at the inlet entrance produced by forebody 1 at acceleration angle-of-attack (α=6°)